

## Pb-free Solder Joint Reliability in a Mildly Accelerated Test Condition

Joe Smetana, Alcatel-Lucent, Plano, TX  
Richard Coyle, Alcatel-Lucent, Murray Hill, NJ  
Thilo Sack, Celestica, Toronto, Canada  
Ahmer Syed, Amkor, Chandler, AZ  
David Love, Oracle, Santa Clara, CA  
Danny Tu, Huawei, China  
Steve Kummerl, Texas Instruments, Dallas TX

### Abstract

Two different temperature cycling profiles were used to compare the thermal fatigue reliability of Pb free and SnPb solder joints in 16 different, high strain surface mount (SMT) packages. In some applications, high strain Pb free (SnAgCu) components are expected to fail earlier than the equivalent SnPb version. In this program, test results were compared for a 0-100°C thermal cycle used often for evaluating high reliability applications to those of a comparatively mild accelerated thermal cycle condition of 20-80°C. A total of 6957 cycles was completed in the 0-100°C testing and a total of 9792 cycles was completed in the 20-80°C thermal cycling. The program was completed after over more than two years of elapsed test time. Weibull analysis, acceleration factors between the tests and failure analysis are included. The results indicate that the SnAgCu (SAC) components that create a high strain in thermal cycling tend to perform worse in 0-100°C testing than identical SnPb soldered components. However, when the strain is reduced by testing with the reduced  $\Delta T$  in the 20-80°C cycle, the SAC thermal fatigue performance is equal to or better than that of identical SnPb soldered components. The encouraging SAC performance in the 20-80°C cycle tends to mitigate Pb free reliability concerns because the lower strain test conditions are closer to actual service conditions.

### Background

Thermal fatigue combined with solder creep is considered the major source of wear out failure of surface mount (SMT) components. Results from several industrial and consortium studies indicate that the thermal fatigue performance of certain types of high strain components is poorer when assembly is done with ternary Sn-Ag-Cu (SAC), Pb-free solder than with SnPb eutectic solder. Significant reductions in Pb free solder joint reliability have been measured in temperature cycling tests, particularly using harsh accelerated conditions such as -40 to +125°C [1-6]. There are similar but less dramatic trends observed using the more common though less severe temperature cycle of 0 to 100°C. Results from the literature also indicate that thermal fatigue performance of Pb free solder is equal to or better than SnPb solder for lower strain components [1,2,4-6,29,30]. High strain components include large ceramic ball grid arrays, ceramic chip resistors, large QFN, and various chip scale package designs (CSP). The thermal fatigue performance of these components is critical because they are used in the majority of high reliability, long life products. Despite progress in recent years [5-28], the significance of the difference in temperature cycling results between high and low strain components has not been determined and there are no accepted acceleration factors or models for SAC reliability that can correlate accelerated conditions to field conditions.

Two key physical characteristics of high strain components are a very large distance to neutral point (DNP) and the large difference in the coefficient of thermal expansion ( $\Delta CTE$ ) between the component and the printed circuit board that occurs after surface mount solder attachment. During temperature cycling, the resultant strain in the component is a strong function of the difference in temperatures extremes ( $\Delta T$ ) of the thermal cycle. These elements of component strain ultimately are manifested as shear strain in the solder joints, which drives thermal fatigue failure of the solder. In simple terms, the solder joint shear strain  $\gamma$  is proportional to the product of the DNP,  $\Delta CTE$ , and  $\Delta T$ :

$$\gamma \propto (\text{DNP}) (\Delta CTE) (\Delta T)$$

The DNP and  $\Delta CTE$  are fixed characteristics of each component but the solder joint strain can be reduced if tested is done with a milder thermal cycle (smaller  $\Delta T$ ). This has significance because lower strain test conditions produce strains that are closer to the strains found in products operating under actual service conditions. It was mentioned previously that the reliability of some high strain components is better with SnPb solder attachment but that the differences between SnPb and SAC may diminish as the severity of temperature cycling conditions diminishes. In the current study, the thermal fatigue performance of several high strain SAC component assemblies is evaluated using both mild and standard thermal cycles. The basic hypothesis for this study is that thermal fatigue performance of high strain SAC assemblies may approach that of comparable SnPb assemblies if the thermal cycling is performed using a milder thermal cycle, one that is closer to actual service conditions. If this proves true, an obvious benefit of such a finding would be to enable the use of existing, accepted

SnPb acceleration factors to estimate the field reliability of SAC. This would represent a conservative interim solution as models for SAC acceleration factors are developed and improved. This approach would be valid for field use environments with a  $\Delta T$  equal to or lower than the  $\Delta T$  used in the mildly accelerated test condition but would not be valid for use conditions characterized by large  $\Delta T$  such as an automotive, under hood environment.

Component availability issues are now driving all segments of the high reliability electronics industry to consider migrating products to Pb free manufacturing. It is acknowledged widely that it will be some time before the industry reaches consensus on predictive reliability modeling for SAC solder. The primary objective of this test program is to provide reliability data immediately that will support business decisions to allow Pb-free products to be introduced into high reliability, long life applications. The test program developed for this study is designed to compare the reliability of high strain components assembled with both SAC and SnPb solder using the common 0 to 100 °C temperature cycle as well as a mildly accelerated temperature cycle that results in lower strain on the components. The minimum expectation is that the SAC reliability can be validated qualitatively with respect to the reliability of SnPb under mildly accelerated, near-use environment conditions.

### Scope of the Test program

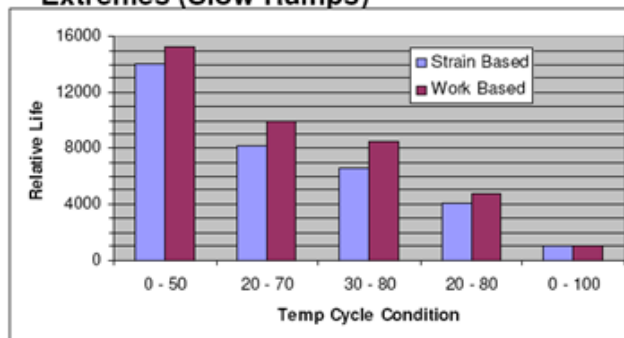
This test program compares the thermal fatigue performance of high strain components using the common 0-100°C accelerated temperature cycling (ATC) test parameters to that of a mildly accelerated temperature cycle that results in much lower strain on the component solder joints. A sample size of sixteen of each component type with SAC solder balls and SAC solder assembly were tested in each of the two thermal cycles. A sample size of thirty two of each component type with SnPb solder balls and SnPb solder assembly were tested in each of the two thermal cycles.

### Choosing the Mild Test Condition

Selecting the parameters for the mild acceleration test condition was a critical element in the project definition. It was essential to establish a balance between ensuring that the test conditions were indeed mild with respect to the 0-100°C test cycle but would provide sufficient acceleration to ensure that the project could be executed in a reasonable time frame. A number of different thermal cycles were proposed for the mild test condition, including 0-50°C, 20-70°C, 30-80°C, and 20-80°C. These were modeled using both creep strain and energy density methods and acceleration factors were estimated for each of the test conditions compared to 0-100°C. The histogram in Figure 1 summarizes the results of the modeling. The modeling results indicate that the 20-80°C thermal cycle is probably the only mildly accelerated test condition that could be completed in a practical timeframe. As an added benefit, the average cycle temperature of 50°C in the 20-80°C cycle is common to the 0-100°C temperature cycle.

## Mild Acceleration Considerations (Predictions)

- Fatigue life dependent on Temperature Range **AND** Temperature Extremes (Slow Ramps)



### Compared to 0 – 100 C cycles

1. 14X higher life for 0 – 50
2. 8X higher life for 20 – 70
3. 6.5X higher life for 30 – 80
4. 4X higher life for 20 - 80

- For the same temp range (50 C), moving the temp extremes up reduces life
- Increasing the temp range by increasing the high temperature reduces life by 2X (20 – 70C VS 20 – 80C cycle)
- Increasing the temp range by lowering the low temperature reduces life by 1.6X (30 – 80C VS 20 – 80C cycle)
- Doubling the range (low temp constant) reduces life by 14X (0 – 50C VS 0 - 100C cycle)

Figure 1: Summary of the Mild Acceleration Test Condition Modeling

The test board was designed to have four each of 13 different component types. The components used in this experiment were all selected to be relatively high strain component types with the SAC assemblies expected to exhibit worse 0-100°C thermal cycle performance than their SnPb counterparts. Table 1 lists the details of the component types, package characteristics, die sizes, and ball sizes.

**Table 1: Description of the component test vehicles**

Part Type	Body Size (mm)	Die Size (mm)	Pitch (mm)	Solder Ball Size (mm)	Comments
CBGA 625	32.5 x 32.5	NA	1.27	0.75	
BGA 192	14 x 14	12.065 X 12.065	0.8	0.46	
BGA 84	7 x 7	5.08 x 5.08	0.5	0.3	
QFN 72	10 x 10	3.2 x 3.2	0.5	NA	Sn finish
QFN 64	9 x 9	7.62 x 7.62	0.5	NA	NiPdAu finish
Meg-Array Connector	44.6 x 17.34	NA	1.27	0.76	300 I/O, 14 mm Height
WSCSP 36	3 x 3	3 x 3	0.5	0.3	
WLCSP 54	9 x 5	9 x 5	0.5	0.35	
Ceramic Oscillator	5 x 7	NA	5.0 x 4.0	NA	
BGA 1936	45 x 45	17.76 x 17.76	1.0	0.6	1 pc. lid
2512 Resistor	NA	NA	NA	NA	
Board Mount Power Supply	50.2 x 46	NA	4.0	NA	Solder Bumped pads 3.2 x 2.2 mm

Test boards were built using a filled phenolic FR4 material with a high glass transition temperature,  $T_g$ . The solderable surface finish was immersion silver (ImAg). The dimensions of the six layer test boards were 10.8 x 16x 0.125 inch (274.3 x 406.4x3.175mm). The 0.125 inch thickness was chosen to increase the stiffness of the soldered structures, which transfers stress to the solder joints more effectively. This was done in an attempt to reduce the time to failure and total test duration, given the much lower acceleration factor of the 20-80°C test. The majority of the daisy chain routing was done on external layers to ensure that via reliability did not impact the continuity of the solder joint daisy chains. When vias were required in the daisy chain nets, large vias were used to reduce the risk of via failure. All the larger pitch ball grid arrays included a through via pattern, non-functional, between the pads to represent a realistic design configuration. Each component was isolated on an “island” in the board to enable individual removal without having to remove an entire assembly. Each island included test points so that individual components could be probed separately. A populated test board is shown in Figure 2.

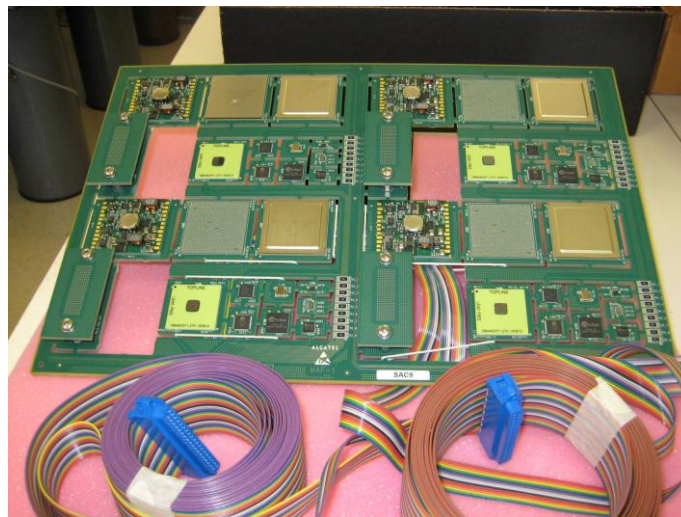


**Figure 2: Fully populated test board. The ribbon cables are used for temperature cycle monitoring Surface Mount Assembly**

Prior to the start of assembly incoming inspection was performed on all the components. Several components had residue or contamination on the balls that could not be readily removed. The affected components were noted in the event of resulting assembly defects or early failures during ATC. For the Pb-free boards a SAC305 alloy paste was used and for SnPb the standard eutectic paste was used. Once assembly was completed, all the boards were run through visual and 5DX x-ray inspection.

Only two significant assembly issues were observed. The CBGA625 and WSBGA54 devices exhibited voiding in excess of that allowed by IPC-610D [29]. X-ray images of the voiding are shown in Figure 3. The root cause of the solder voiding is believed to be due to contamination during BGA ball attachment. There were several instances of insufficient solder on the 0.5mm pitch BGA84 device as shown in Figure 4. The root cause of the insufficient solder is believed to be due to the paste type and stencil thickness used for the build. These defects were noted in the attachment defect reports for later cross referencing to ATC failure data.

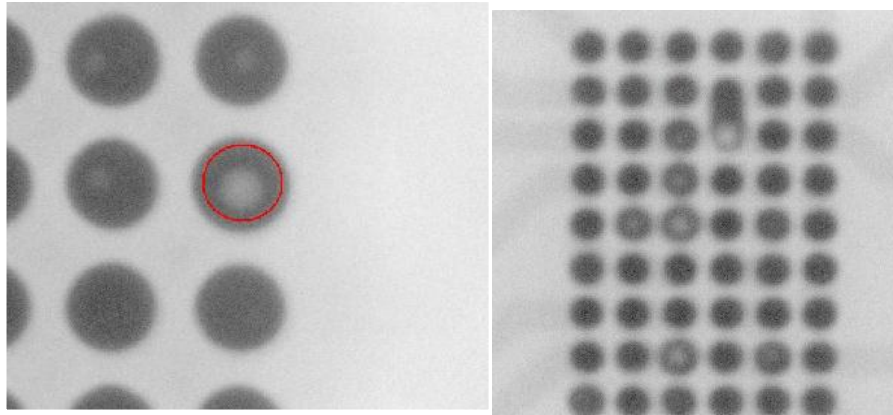


**Figure 3: Excessive Voiding Levels on CBGA625 and WSBGA54 Devices after Reflow**

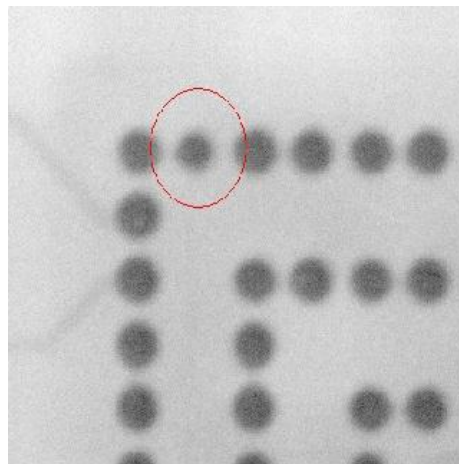


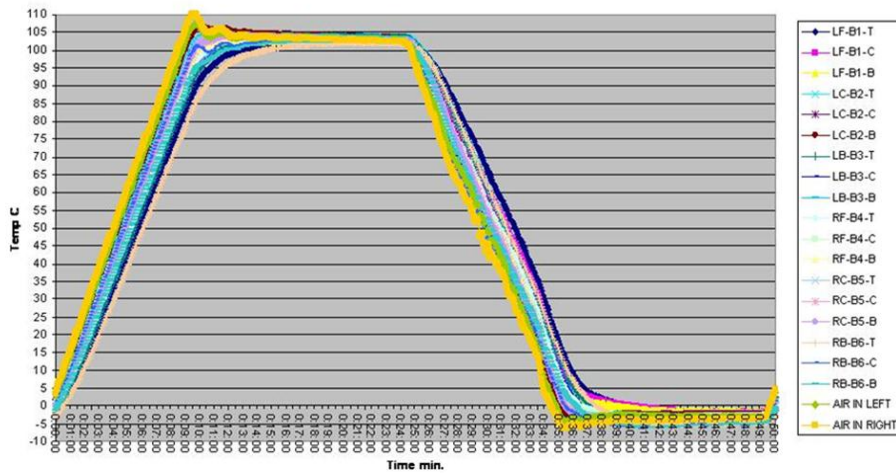
**Figure 4: Example of Insufficient Solder on 0.5mm Pitch BGA84 Component**

#### **Accelerated Temperature Cycling (ATC)**

The thermal cycling profiles for the 0-100 °C and 20-80 °C tests are shown in Figures 5 and 6 respectively. The 0-100 °C test profile used 15 minute ramp times and 30 minute hot and cold dwell times. The 20-80 °C test used 25 minute ramp times and 30 minute hot and cold dwell times. The relatively slow ramp times were necessary to ensure that the wide range of component sizes and types on the test board would experience approximately the same thermal profile.

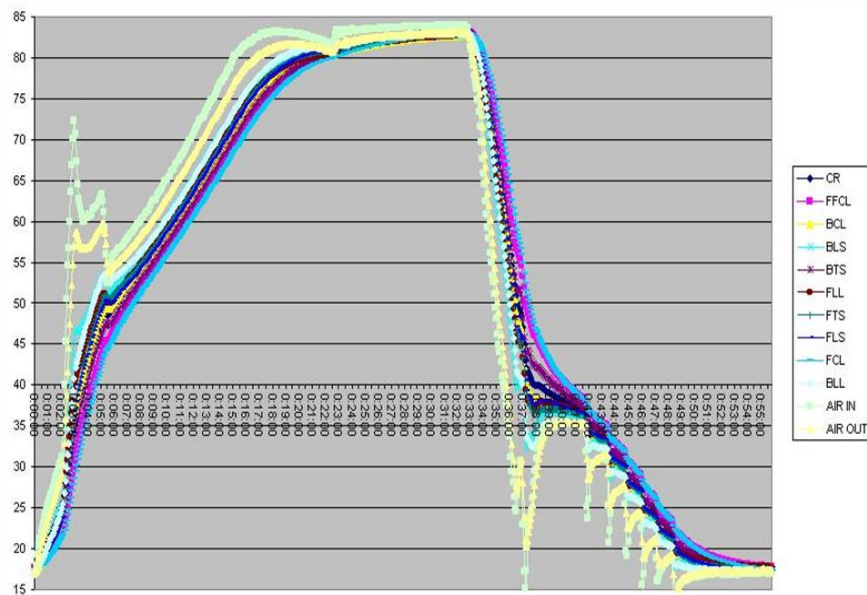
The components and the test circuit boards were daisy chained to allow electrical continuity testing after surface mount assembly and in situ continuous monitoring during thermal cycling. The resistance of each loop was independently monitored during the temperature cycle test. All assembled circuit boards were thermally cycled from 0 °C to 100 °C with a 10 minute ramp between temperature extremes. Aside from using extended ramp times, the thermal cycling was done in accordance with the IPC-9701A industry test standard [30]. The solder joints were monitored continuously during thermal cycling with

event detectors set at a resistance limit of 1000 ohms. A spike of 1000 ohms for 0.2 microseconds followed by 9 additional events within 10% of the cycles to the initial event is flagged as a failure. The failure data were reported as characteristic life  $\eta$  (number of cycles to 63.2% failure) and slope  $\beta$  from a two-parameter Weibull analysis.



30 minute dwells with 15 minute ramps (90 minute cycle time)  
(above has shortened dwell just for setting up chamber)

**Figure 5: Thermal profile for the standard 0-100°C accelerated temperature cycle**



25 minute dwells and 30 minute ramps, 110 minute total cycle time

**Figure 6: Thermal profile for the mildly accelerated 20-80°C temperature cycle**

### Temperature Cycling Results - Weibull and Regression Analysis

The 0-100 °C test was terminated after 6957 cycles and the 20-80°C test was ended after 9792 cycles. The total cycling time was approximately 14 months for the 0-100 °C testing and was slightly over two years for the 20-80°C testing. It is uncommon to see such extended ATC test durations and more over, these tests were performed using components and a test board that were expected to generate failures in comparatively short test intervals.

Extensive Weibull and regression analysis was completed on the failure data. A summary of the thermal cycling performance for all of the components in each temperature cycle is shown in Table 2. The following interesting observations can be made regarding some overall trends in the thermal cycling data.

- **The SnPb solder did not unilaterally outperform the SAC solder in 0-100 °C testing as might be expected for high strain components.** The highlighted eta (characteristic lifetime) cells in Table 2 for the 0-100 °C test show

that only four of the high strain components exhibit poorer performance with SAC compared to SnPb assembly and one of those, the QFN72, had only marginally lower reliability (~ 4%).

- **Collectively, the 20-80°C results confirm the working hypothesis that thermal fatigue performance of high strain SAC assemblies approaches that of comparable SnPb assemblies when the thermal cycling is performed using a milder thermal cycle.** The highlighted eta cells for the 20-80°C testing show that only two of the high strain components, the QFN64 and the 5x7 ceramic oscillator, exhibit poorer performance with SAC solder. In the case of the 5x7 oscillator, the reliability measured by characteristic lifetime of the SAC is not significantly lower than the SnPb (~ 3% difference).
- **There is a wider distribution of data in the 0-100°C testing of SAC solders as reflected in lower Weibull beta values.** The same effect was not seen in the case of the 20-80°C data, where the strain levels are lower. This suggests that in higher strain or higher peak temperature conditions, SAC solder has more variability in the performance in thermal cycling than Pb-free, but in lower strain or lower peak temperature conditions, the variability seen in ATC performance is similar.
- **For the BGA components evaluated in this study, the SAC characteristic life is always better than SnPb.** This is an important finding since there is widespread industry concern regarding the reliability of ball grid arrays with SAC solder. The uncertainty of BGA reliability with SAC solder is considered by many to be an obstacle to the Pb free transition.

More detailed discussions of the temperature cycling results are presented by individual components in the subsequent sections.

**Table 2: Summary of thermal cycle performance**

Data though 6957 cycles of 0-100C (and completed) and through 9792 cycles of 20-80C (and completed)												
Note - Early Fails are NOT included in this data												
Component	Failure Distribution Characteristics (excluding any early fails)											
	SnPb 0-100 °C			SAC 0-100 °C			SnPb 20-80 °C			SAC 20-80 °C		
	Eta	Beta	FFT	Eta	Beta	FFT	Eta	Beta	FFT	Eta	Beta	FFT
2512	1804	11.34	NA	1588	7.647	NA	4284	3.922	NA	7094	12.35	NA
5x7	2541	7.746	1730	1831	6.186	954	6703	3.366	764.5	6453	7.698	2797
BGA192	1773	30.66	NA	2554	7.308	NA	3296	13.28	NA			NA
BGA1936	5320	8.645	NA	1 Fail	NA	NA	9442	6.64	NA			NA
BGA84	3146	11.91	NA	5058	10.64	NA	7457	10.14	NA			NA
BMPS	0 Fails	NA	NA	0 Fails	NA	NA			NA	1 fail		NA
CBGA	Voided	Voided	Voided	Voided	Voided	Voided	Voided	Voided	Voided	Voided	Voided	Voided
Meg-Array	6407	3.377	NA	9584	1.485	NA	8370	7.025	NA			NA
QFN64	565	4.609	NA	163	1.836	NA	1481	4.08	NA	1171	6.594	NA
QFN72	5300	66.07	NA	5114	4.796	NA			NA			NA
WSBGA36	2135	12.98	NA	2208	11.34	NA	4459	8.448	NA	7795	7.392	NA
WSBGA54	2027	2.246	NA	2385	2.555	NA	4773	2.704	NA	12964	1.963	NA
Average	3240.55	15.81	1730.00	3387.22	5.98	954.00	5585.00	6.62	764.50	5628.25	7.20	2797.00
										WSBGA54 Eta Excluded		

Light Green = increase in Eta or FFT compared to SnPb

Pink = decrease in Eta or FFT compared to SnPb

Yellow = decrease in Beta compared to SnPb

Green = increase in Beta compared to SnPb

2512 Resistor

Figure 7 shows the Weibull plots of the failure data for the 2512 resistor in both thermal cycles. There was an early failure in the 20-80°C thermal cycle testing. The data is analyzed both with and without the early failure. This was one of the components that met the expectation for the SnPb performance to exceed the SAC performance in the 0-100°C thermal cycle. In the 0-100°C thermal cycling, the beta value (slope of the plot, reflecting the spread of the distribution) is significantly higher for SnPb than it is for SAC. In the 20-80°C thermal cycling, the result is reversed for this component, with the SAC assembly outperforming the SnPb assembly by a substantial amount.

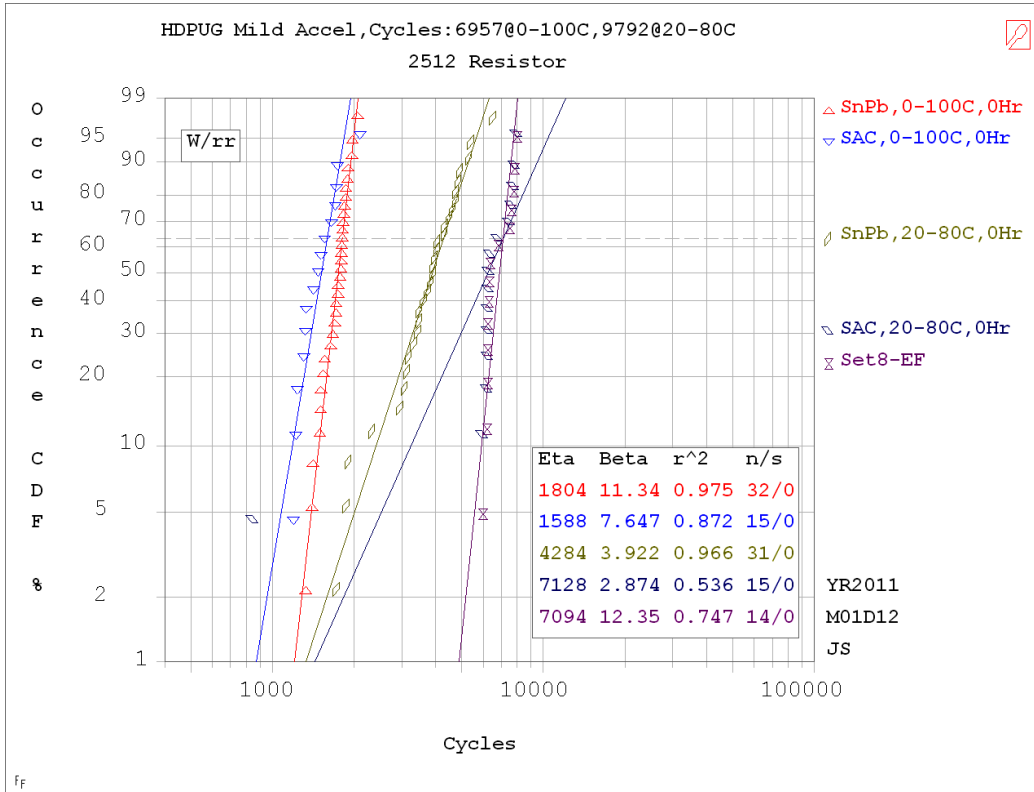


**Figure 7: Weibull plots of the 2512 resistor thermal cycle failures**

5 x 7 mm Ceramic Oscillator

Figure 8 shows the Weibull plots of the failure data for the 5 x 7 mm ceramic oscillator in both thermal cycles. This was another one of the components that met the expectation for the SnPb performance to be better than SAC performance in the 0-100°C thermal cycle. In the 20-80°C thermal cycle testing, based on characteristic life, the SnPb assembled component still outperformed the SAC assembled components, but the difference is less than 15% and the differences in the characteristic lives are not statistically different at the 95% confidence level. However, the slope (beta) of the distribution for the SnPb assembled components in the 20-80°C thermal cycle testing is dramatically less, such that the first failures for the SnPb assembled components are much earlier than the SAC assembled components.

The shape of the 0-100°C distributions on the 2-parameter Weibull plot is clearly a curve. Only the SnPb, 20-80°C failure distribution is a good fit to a 2 parameter Weibull distribution. Statistically the three other distributions are a better fit to a 3-parameter Weibull distribution. This same data is plotted as 3-parameter Weibull data, including the 90% confidence intervals, in Figure 9. This clearly shows, based on failure free time, that in the 20-80°C thermal cycle the SAC assembled devices outperform the SnPb assembled devices. One of the interesting items here is that the failure free time for the SnPb assembled package in 20-80°C is less than for 0-100°C. In fact, no matter how the data is analyzed (2 parameter or 3 parameter) the SnPb first fails in 20-80°C thermal cycling are, at best, only marginally better than the performance in 0-100°C thermal cycling.

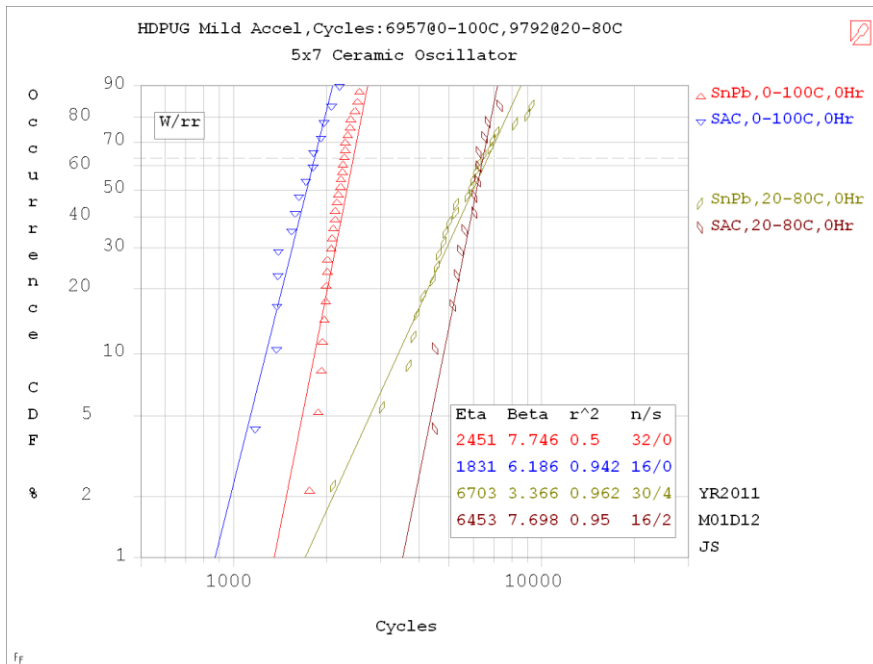


Figure 8: Weibull plots of the 5 x 7 mm ceramic oscillator thermal cycle failures

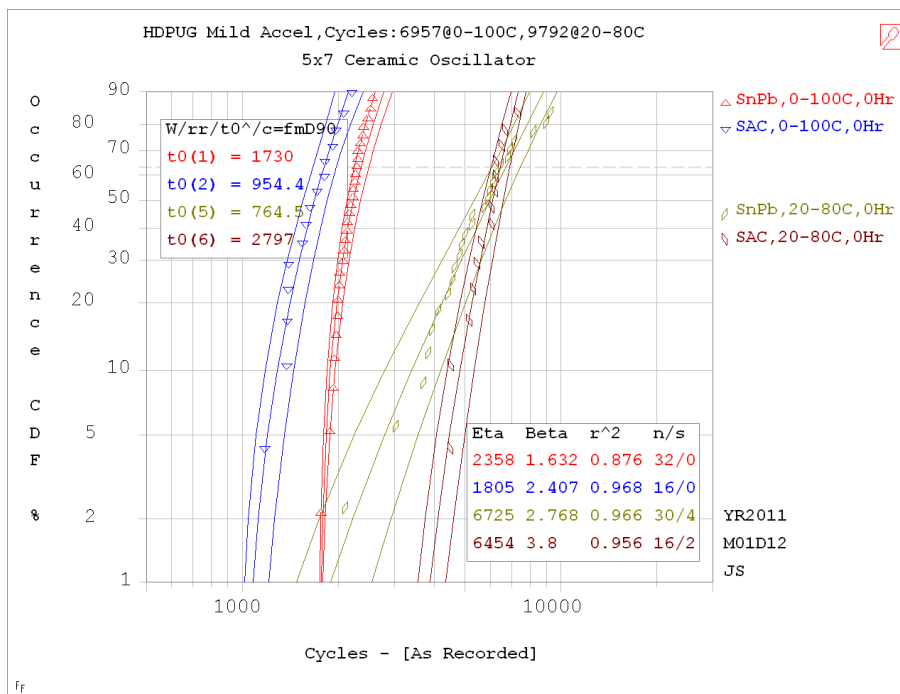


Figure 9: 3-parameter Weibull plots of the 5 x 7 mm ceramic oscillator thermal cycle failures

BGA 192

Figure 10 shows the Weibull plots of the failure data for the BGA 192 in both thermal cycles. Based on characteristic life, this component did not meet the expectation for the SnPb component to outperform the SAC components in the 0-100°C thermal cycling. However, if this data is evaluated looking at the 1% failure rates, rather than the characteristic life, then SnPb outperformed SAC, as the beta values (slopes) of the distributions for the SAC BGA failure data are consistently and considerably lower than that for SnPb. In the 20-80° thermal cycling, the SAC BGA clearly outperformed the SnPb BGA, though this cannot be fully quantified due to the absence of SAC failures in the 20-80°C thermal cycle test.



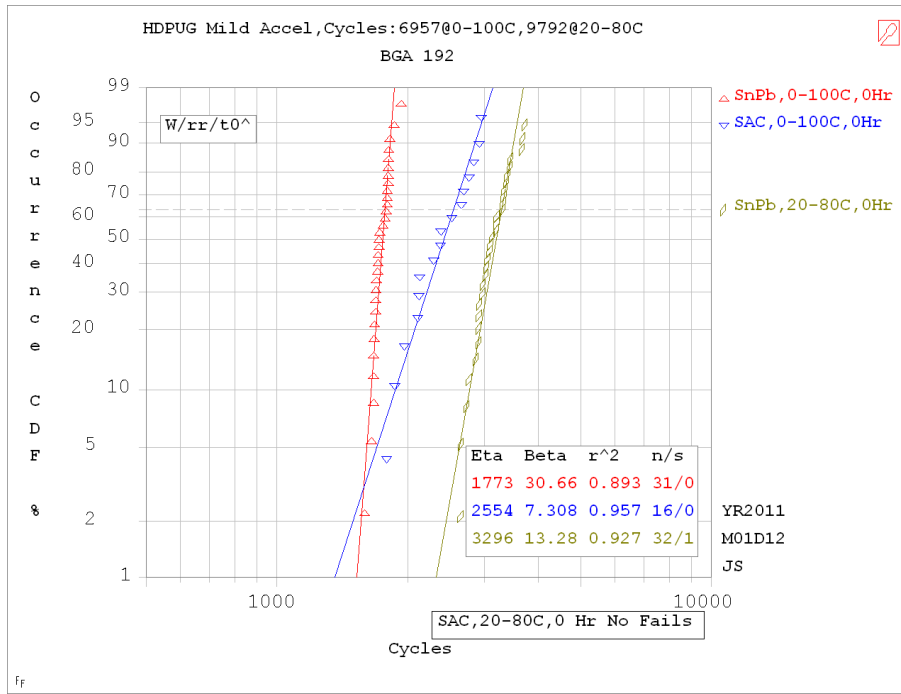


Figure 10: Weibull plots of the BGA 192 thermal cycle failure data

BGA 1936

Figure 11 shows the Weibull plots of the failure data for the BGA 1936 in both thermal cycles. The SAC BGAs outperform SnPb BGAs in both thermal cycle conditions. In the 0-100°C thermal cycling, there were very few SAC failures.

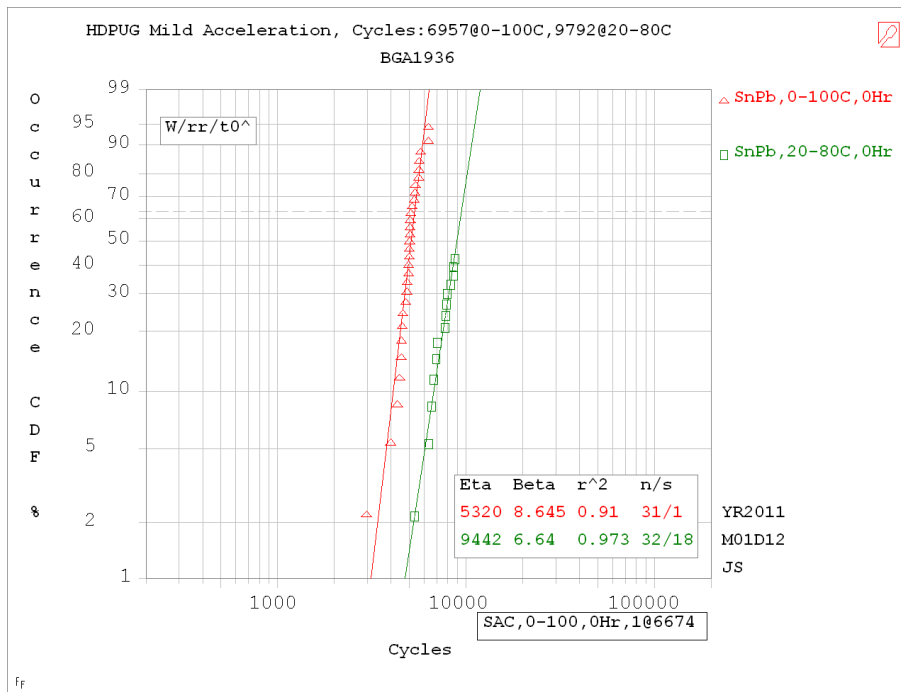
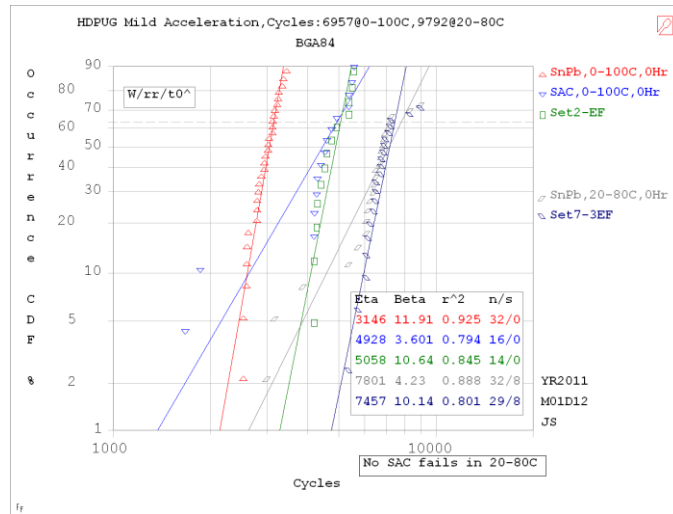


Figure 11: Weibull plots of the BGA 1936 thermal cycle failure data

BGA 84

Figure 12 shows the Weibull plots of the failure data for the BGA 84 in both thermal cycles. There are no SAC failures in the 20-80°C thermal cycling. There are a number of “early” fails in this data, and the data is analyzed both with and without these early fails. The early fails in the SAC BGAs in the 0-100°C thermal cycling distribution are at over 1000 cycles. These may or may not be manufacturing related failures. These are all very small solder joints and minor variability could make a major difference in the reliability. For this distribution the statistical probability of competing failure distributions is small.

It is more likely that these are separate distributions or could be manufacturing related failures. Also note that the statistical fit of these distributions is poor even when early fails are removed. The SnPb distribution in the 20-80°C thermal cycle data is not a good statistical fit to a Weibull distribution with or without the early failures included and in fact is a better fit with the early failures included. When you ignore the early fails, SAC clearly outperforms SnPb regardless of preconditioning in both the 0-100°C and the 20-80°C thermal cycles.



**Figure 12: Weibull plots of the BGA 84 thermal cycle failure data**

**BMPS**

The BMPS device had no failures. No Weibull plots are possible, and no further analysis is planned.

**CBGA 625**

Figure 13 shows a cross-section of severe solder voiding at the interface where the ball is attached to the ceramic CBGA 625 package interface. This voiding badly compromised the cycling data for this component. No further analysis is planned.

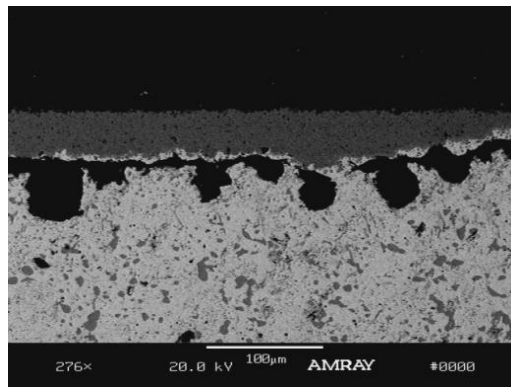


**Figure 13: A photomicrograph showing significant solder voiding at the interface where the solder ball is attached to the ceramic substrate.**

**Meg-Array Connector**

Figure 14 shows the Weibull plots of the failure data for the Meg-Array mated connector pair in both thermal cycles. It was difficult to get a clean data set on this connector pair in the 0-100°C thermal cycling. There were early failures in this data and the data has been plotted both with and without them, with a best guess as to where to distinguish between early failures and the wear-out distribution(s). However, it is clear that there are two failure modes in the SAC 0-100°C data as seen in Figure 15. This second failure mode is also still there after removing the early failures. This may or may not also be showing up in the other conditions. The 20-80°C data did not have any problems with early failures and only the SnPb assemblies failed in this thermal cycle condition. In 0-100°C thermal cycling, it is difficult to state which condition (SnPb or SAC) really performed better as it is a function of how the data is analyzed (characteristic life or 1% failure rate), and whether or not the early failures are included in the analysis. Also, in the 0-100°C thermal cycling, the slopes of the Weibull plots (beta) are low, even with the early failures removed. SAC assemblies clearly outperformed the SnPb assemblies in the 20-80°C thermal cycling.

One unusual result in this data is that the characteristic life of the SnPb assembly in 20-80°C thermal cycling is less than 20% better than the characteristic life of this assembly in 0-100°C. This is a very small acceleration factor between these two test conditions.

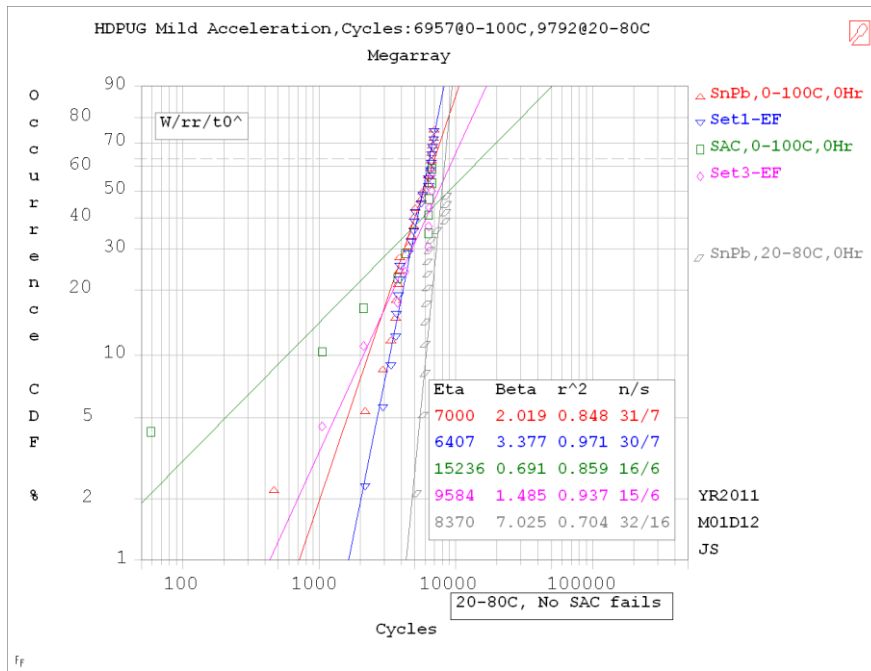


Figure 14: Weibull plots of the Meg-Array connector pair thermal cycle failure data

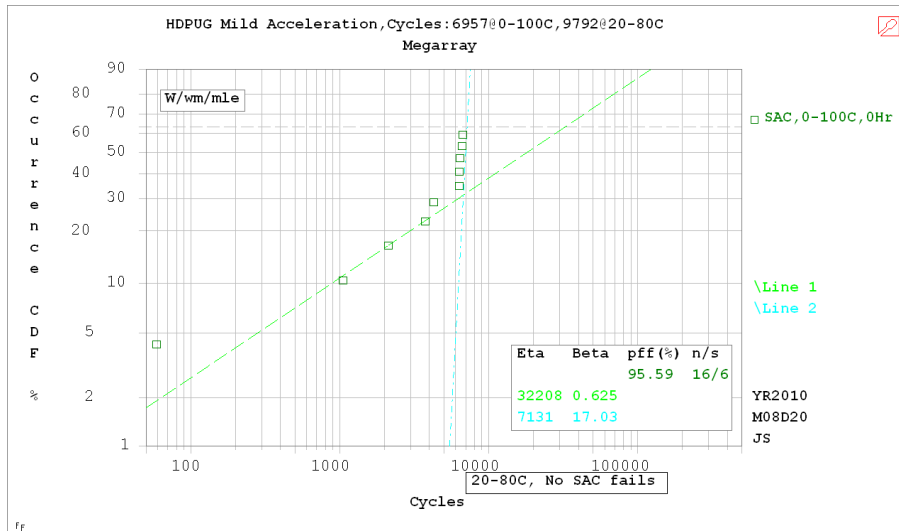


Figure 15: Mixed mode analysis showing a high probability of a 2<sup>nd</sup> failure mode in the SAC 0-100°C thermal cycling.

QFN64

Figure 16 shows the Weibull plots of the failure data for the QFN 64 in both thermal cycles. SnPb clearly outperforms SAC in the 0-100°C thermal cycle test. In the 20-80°C thermal cycle test, SnPb performance is still better. However, the relative performance of SAC is much closer to that of SnPb in this thermal cycle than it is in 0-100°C. Low Weibull beta on the SAC assembled QFN is consistent with other published results on large die 9x9 QFN's [3]. This greatly reduced slope and resulting poor performance is almost surely a result of a different failure mode. Note that this component has a very large die to package ratio.

The very low Weibull slope seen in SAC 0-100°C thermal cycle is not repeated in 20-80°C thermal cycling. The failure data in the 20-80°C thermal cycling is also a better statistical fit to a 3 parameter Weibull as shown in Figure 17.

This is not the case in 0-100°C thermal cycling which is expected considering how quickly these devices failed. This correlation to a 3 parameter Weibull is also consistent with the results on the 5 x 7 mm ceramic oscillator package reported earlier, which is also a flat, no lead, low CTE package.

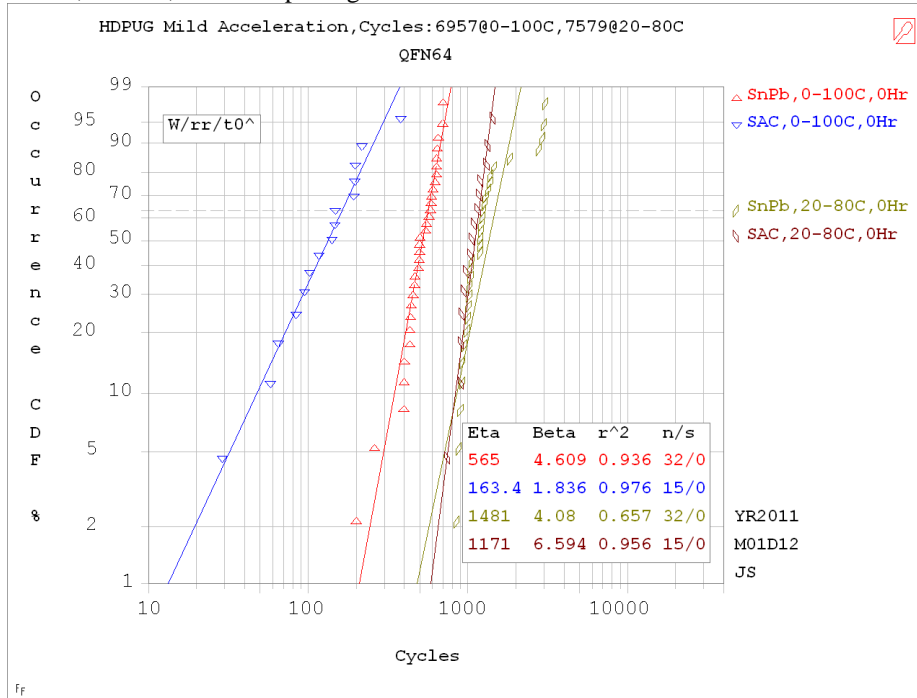


Figure 16: Weibull plots of the QFN 64 thermal cycle failure data

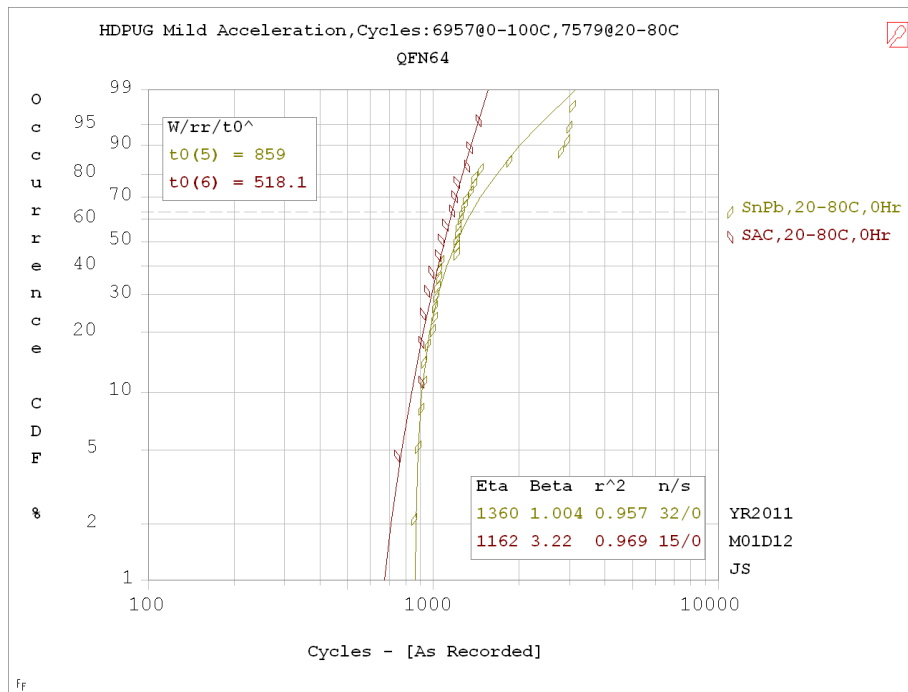


Figure 17: 3 Parameter Weibull plots of the QFN 64 failure data in 20-80°C thermal cycling

QFN 72

Figure 18 shows the Weibull plots of the failure data for the QFN 72 in both thermal cycles. SnPb clearly outperforms SAC in the 0-100°C test range. In the 20-80°C thermal cycle testing, the result is exactly the opposite, with SAC outperforming SnPb. SAC soldered QFNs appear to have early failures, and the data is analyzed both with and without these early failures. However, these failures are clearly indicated as a second failure mode as shown in Figure 19 and the full data set is mixed mode.

The second failure mode could be similar to what was seen for the QFN 64 shown above or less likely could be manufacturing related. The die to package ratio for this QFN 72 is not as large as the QFN 64, but may be large enough to induce the same failure mode.

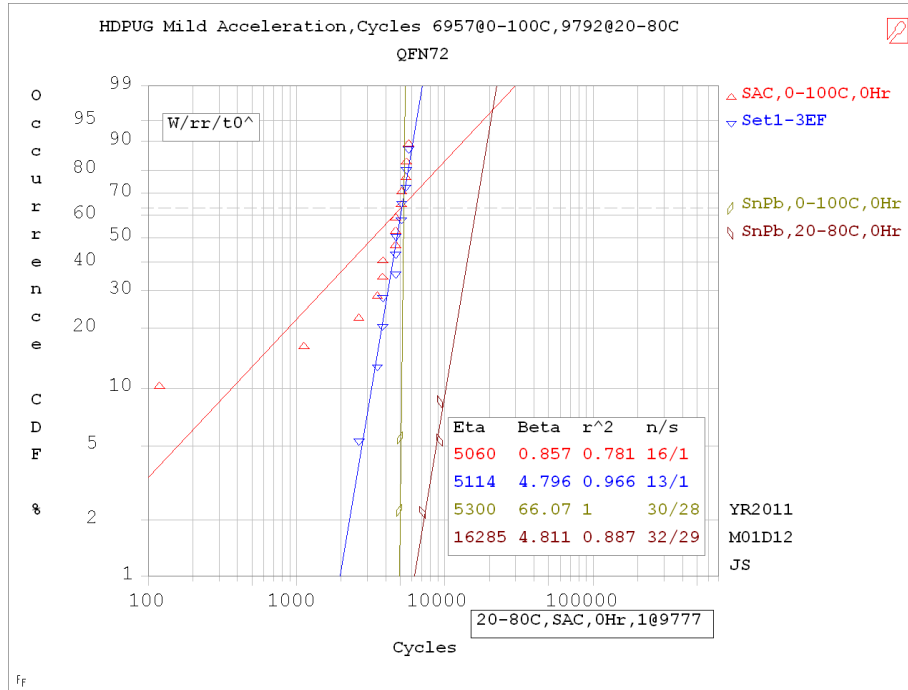


Figure 18: Weibull plots of the QFN 72 thermal cycle failure data

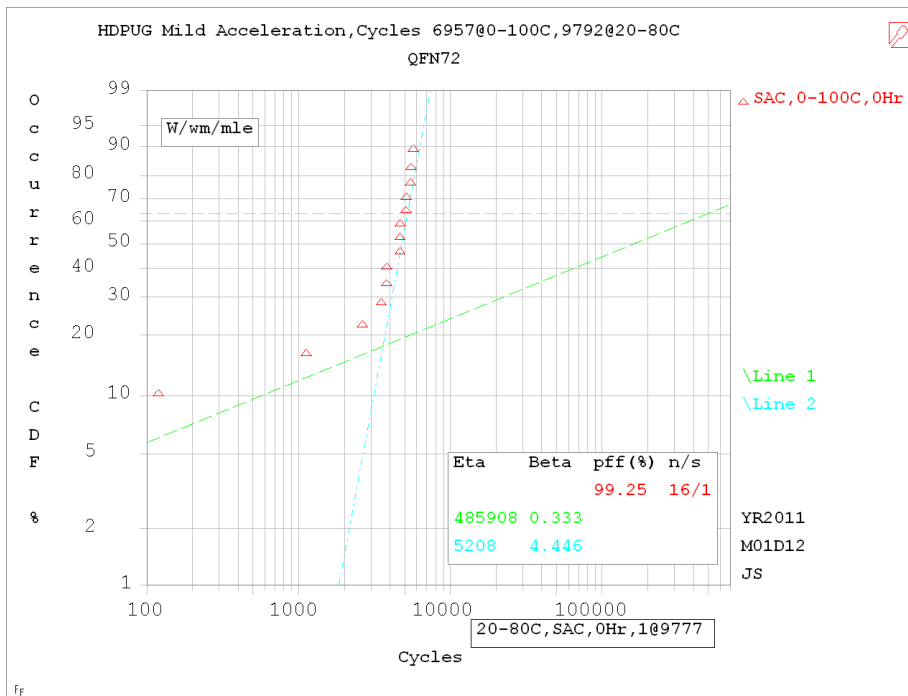


Figure 19: Mixed Mode analysis of the failure data for the SAC QFN 72 in 0-100°C thermal cycling.

WSBGA 36

Figure 20 shows the Weibull plots of the failure data for the WSBGA 36 in both thermal cycles. This data has what appear to be early failures in 0-100°C thermal cycling for both the SAC and SnPb cases. As with other early failures they could be manufacturing related or evidence of another failure mode. The “early failures” could be similar to the failure mode seen on the QFN64. Mixed mode analysis as shown in Figure 21 for this thermal cycle suggests additional failure modes rather than manufacturing related defects. In any case, the data has been analyzed and plotted both with and without the early failures..

Ignoring the early failures on the SAC distributions, then SAC and SnPb assemblies perform very similarly in 0-100°C thermal cycling. In 20-80°C thermal cycling SAC assemblies clearly outperform SnPb.

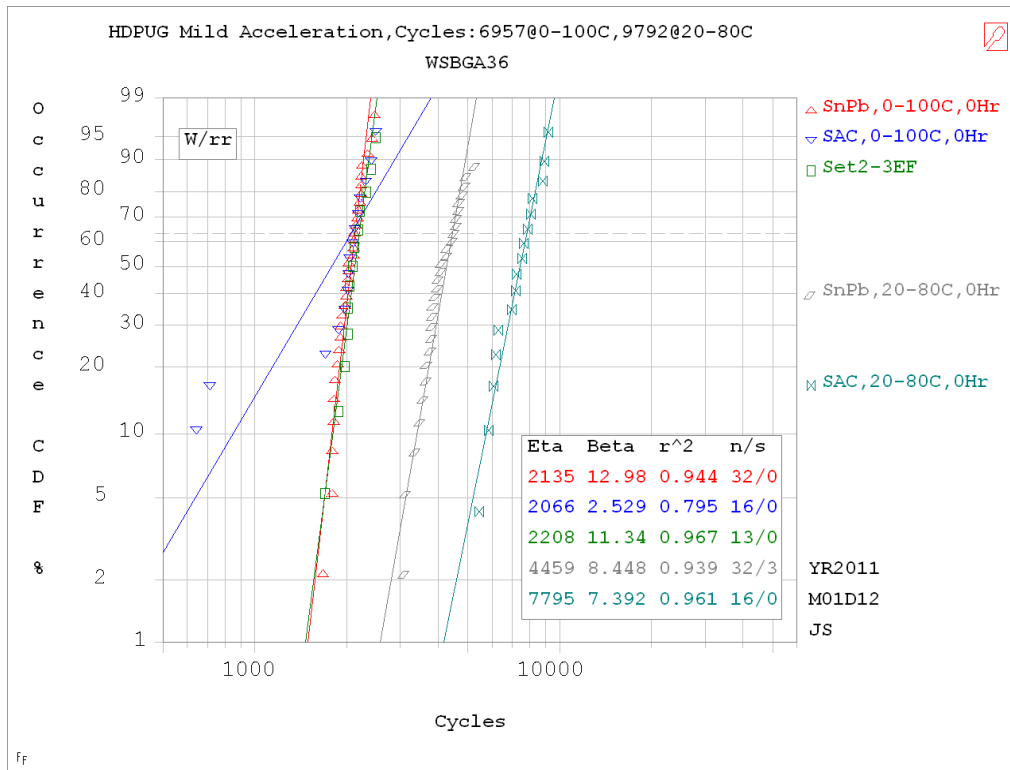


Figure 20: Weibull plots of the WSBGA 36 thermal cycle failure data

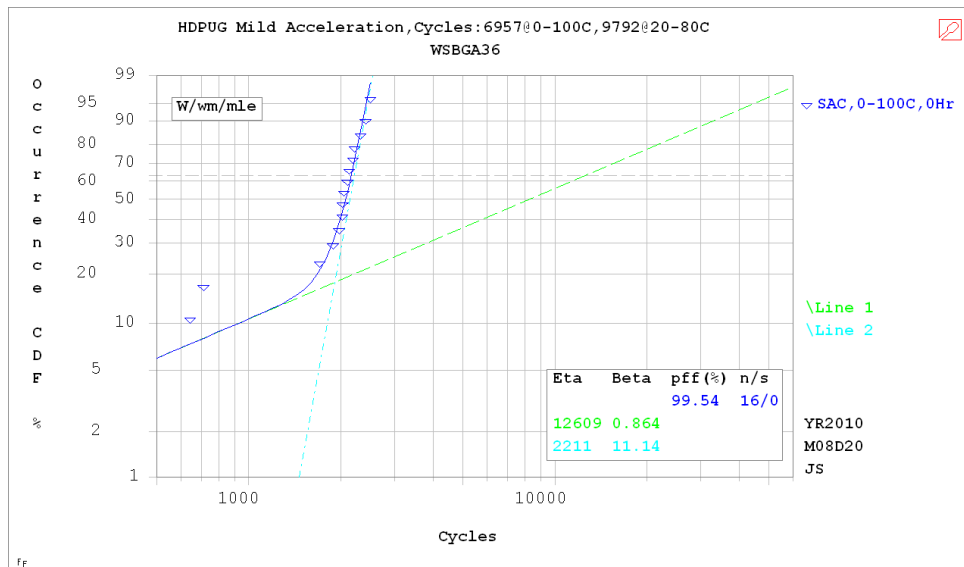


Figure 21: Mixed mode analysis on failure data for the WSBGA 36 in 0-100°C thermal cycling for the SAC assembly.

WSBGA 54

Figure 22 shows the Weibull plots of the failure data for the WSBGA 54 in both thermal cycles. Note that the SnPb BGAs were re-balled from SAC BGAs and there were a number of manufacturing defects clearly associated with the reballing procedure. These have been removed from the data, thus the sample sizes are smaller than typical for the SnPb components. The Weibull plots for this component generally show low Beta values (<3). Based on the characteristic life, SAC outperforms SnPb on this part.

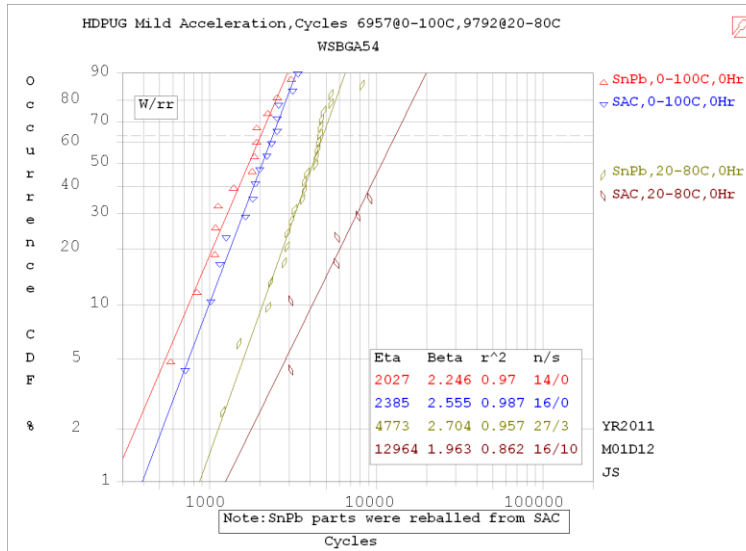


Figure 22: Weibull plots of the WSBGA 54 thermal cycle failure data

**Acceleration Factor Calculations**

Table 3 summarizes the acceleration factors calculated from the test data of the 0-100°C and 20-80° thermal cycling. This table shows comparisons of characteristic life and 1% failure rate. For the 5 x 7 oscillator, the 3 parameter Weibull failure free time is also used to calculate an additional acceleration factor. Data in red is excluded from the averages due to various anomalies in the individual component data that skew these results as discussed in the individual Weibull analyses. The data in this table does not include early failures. Although there is a significant spread in the acceleration factor data, the SAC acceleration factors consistently are considerably greater than the SnPb acceleration factors, regardless of the method used for the calculation. The average acceleration factors for SAC are roughly 3 to 4 compared to approximately 2 for SnPb.

**Table 3: Summary of Acceleration Factors**

Data though 6957 cycles of 0-100C and through 9792 cycles of 20-80C						
Note - Early Fails are NOT included in this data						
	Acceleration Factors (AF)					
	AF SnPb			AF SAC		
Component	Eta	1%	FFT	Eta	1%	FFT
2512	2.37	1.1	NA	4.46	1.1	NA
5x7	2.7	1.26	0.44	3.52	4.08	2.93
BGA192	1.86	1.53	NA			
BGA1936	1.77	1.51	NA			
BGA84	2.37	2.22	NA			
BMPS	NA	NA	NA	NA	NA	NA
CBGA	Voided	Voided	Voided	Voided	Voided	Voided
Meg-Array	1.2	11.2				
QFN64	2.62	2.3	NA	7.18	43.7	NA
QFN72						
BGA36	2.1	1.7	NA	3.5	2.84	NA
WSBGA54	2.35	3.3	NA	5.4	3.15	
Average	2.27	1.87	0.44	3.83	2.79	2.93
	Excludes Meg-Array AF	Excludes QFN 64, WSBGA54 Eta AF				

### Failure Analysis

After 2046 cycles of 0-100°C, a number of components were removed from the thermal cycle chamber for failure analysis. The primary goals of this failure analysis were to validate that the prevalent failure modes were not manufacturing related, and hopefully identify the causes for low beta and early failures on the SAC assembled QFN64.

The cross-sections completed did not show any manufacturing defects or anomalies. Typical fatigue failures were found on most cross-sections. See Figures 23-26 for examples. The QFN data confirmed normal assembly and consistent solder joints (for example Figure 27), but unfortunately could not identify a different failure mode in the devices. The failures on this device were all at less than 250 thermal cycles. Additional damage done in the subsequent ~1800 thermal cycles masked any evidence of the original failure mode.



Figure 23: 5x7 Ceramic Oscillator, assembled with SAC solder, failed at 1586cycles in 0-100°C thermal cycling.

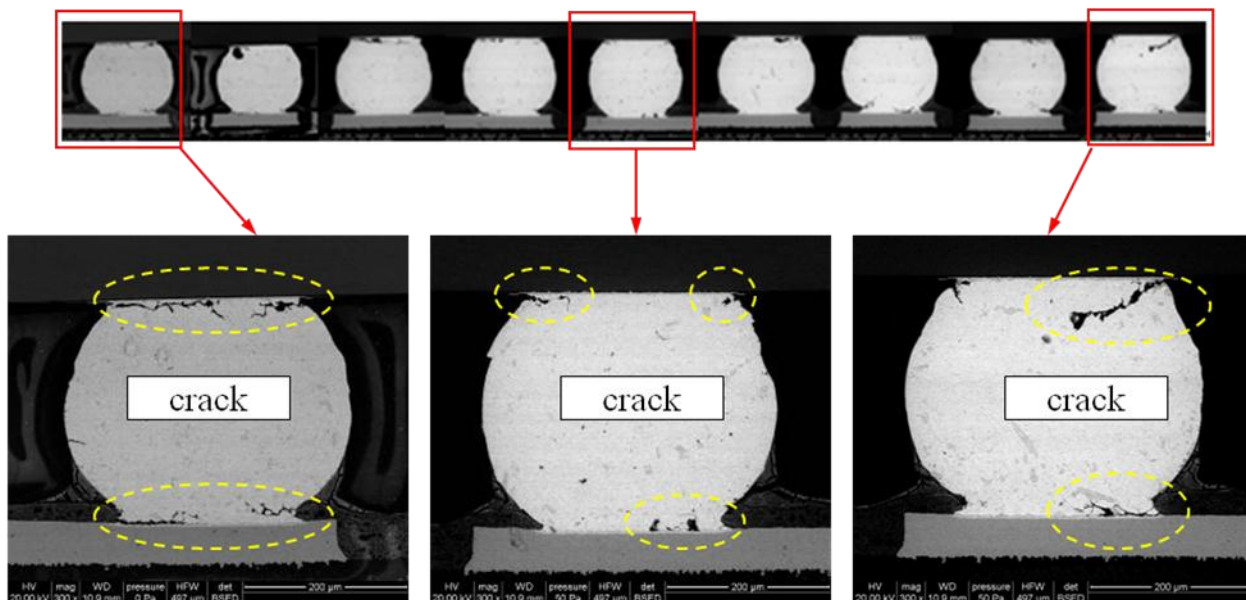
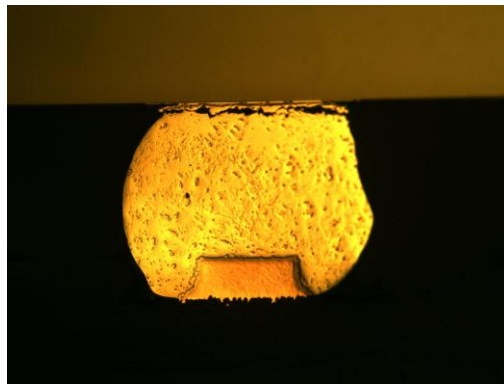
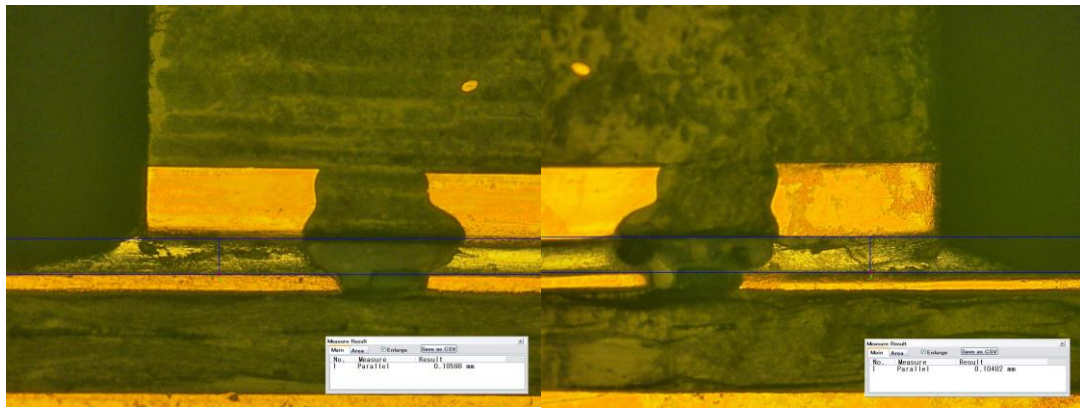


Figure 24: WSBGA 54, assembled with SAC solder, failed at 1639 cycles in 0-100°C thermal cycling.





**Figure 25: WSBGA 36, Assembled with SAC solder, failed at 1886 cycles in 0-100°C thermal cycling**



**Figure 26: QFN64, Assembled with SAC solder with failure at 84 cycles in 0-100°C thermal cycling**

### Summary

The results from the mild acceleration, 20-80°C thermal cycling tests indicate that the thermal fatigue performance of the high strain SAC (Pb free) components is equal to or better than that of identical SnPb soldered components. This confirms the hypothesis that the reliability of SAC assemblies approaches that of comparable SnPb assemblies when tested using a mildly accelerated thermal cycle. This is a very beneficial finding because it suggests strongly that SAC and SnPb solders have comparable thermal fatigue reliability under test conditions approaching certain high reliability service environments such as those found in telecommunication applications. Further, this finding enables the use of existing SnPb acceleration factors to provide a conservative estimate of the field reliability of SAC pending development of better SAC predictive models.

### Conclusions

The following specific conclusions can be drawn from the results of the thermal cycling study:

- The SnPb solder did not unilaterally outperform the SAC solder in 0-100 °C testing as might be expected for high strain components.. This suggests that the reliability of SAC is not substantially worse than SnPb for many components, even when testing is done with the 0-100 °C.
- The 20-80°C test results confirm the working hypothesis for this project that thermal fatigue performance of high strain SAC assemblies approaches that of comparable SnPb assemblies when the thermal cycling is performed using a milder thermal cycle. Only two of the high strain components, the QFN64 and the 5x7 ceramic oscillator, exhibited poorer performance with SAC solder and in the case of the 5x7 oscillator, the reliability of the SAC is not measurably lower than the SnPb (~ 3% difference).
- The SAC characteristic life is always better than SnPb for all the BGA components evaluated in this study. This is an important result because of the long standing concern regarding the reliability of SAC ball grid arrays. Adequate BGA reliability with SAC solder is vital to the successful transition to Pb free design and manufacturing.
- In view of the aforementioned conclusions, SnPb acceleration factors should enable a conservative estimate of performance when used on data generated at 0-100°C as long as the thermal cycle end use environment is no more severe than 20-80°C. This conclusion provides a path to confirming the reliability of Pb free product designs.

- A wider distribution of data, and associated lower Weibull beta for SAC was found in the 0-100°C testing. The same effect was not seen in the 20-80°C data, where the strain levels were lower. This suggests that conditions of higher strain or higher peak temperature lead to more variability in SAC thermal cycling performance than in SnPb. However, with conditions of lower strain or lower peak temperature, the variability seen in thermal cycling performance of the two solders is similar.
- The statistical analysis suggests that a second failure mode may be present in at least one component (and possibly a few others). The indication is that the second failure mode occurs with 0-100°C thermal cycling but does not occur with the 20-80°C thermal cycling. Failure analysis was not successful in identifying the actual failure mode and further work is suggested to study this behavior.

### Suggestions for Additional Work

This work focused on the differences between 0-100°C temperature cycling and 20-80°C temperature cycling on the thermal fatigue reliability of SnPb and SAC solders. There was one significant item identified whose root cause could not be identified. There appears to be a different failure mode exhibited by large die QFN in the 0-100°C thermal cycle that is not observed in the 20-80°C thermal cycle. If a different mode arises as temperature cycling conditions become more severe, a project specifically designed to understand this issue would be particularly valuable for those with severe end use application environments such as automotive and military aerospace.

### Acknowledgements

The authors would like to recognize the overall program support from the High Density Packaging User Group consortium and HDPUG Director, Marshall Andrews. They also acknowledge the management support of Marc Benowitz and Sherwin Kahn from Alcatel-Lucent Bell Labs Reliability and the technical expertise of Richard Popowich of Alcatel-Lucent for his conscientious laboratory support over the more than two year period required to complete the temperature cycling. Special thanks also are extended to Teng Hoon Ng, Dussanee Chanwiboon, and Theeraphong Kanjanupathum of Celestica-Thailand for performing the surface mount assembly and quality inspections.

### References

1. Jean-Paul Clech, "Lead-Free and Mixed Assembly Solder Joint Reliability Trends", Proceedings of IPC/APEX, 2004.
2. Jefferey C. Suhling, H.S.Gale, Wayne Johnson, M. Nokibul Islam, Tushar Shete, Pradeep lall, Michael J. Bozack, John L. Evans, Ping Seto, Tarun Gupta, James R. Thompson, "Thermal Cycling Reliability of Lead Free Solders for Automotive Applications", Inter Society Conference on Thermal Phenomena, 2004, pp. 350-357.
3. Alex Chan, Aman Kahn, Robert Kinyanjui, "Second Level Solder Joint Reliability of Quad Flat No-Lead (QFN) Packages for Use in IPC Class-2 Assemblies", SMTAI, Orlando, 2007
4. Amit Shah, Saketh Mahalingam and Kunal Goray "Reliability Evaluation of Lead Free Electronics for Automotive Applications", CARTS USA, April 2006, Orlando, FL. Ahmer Syed, "Reliability of Lead-Free Solder Connections for Area-Array Packages", IPC/APEX, 2001.
5. Chaillot, M. Grieu, C. Munier, I. Lombaërt-Valot, S. Bousquet, C. Chastanet, J-P. Canaud, R. Dumonteil, S. Villard, P. Raynal, D. Maron, "Fatigue life prediction models developed for Green Electronics in Aeronautical and Military Communication Systems (GEAMCOS)", Proceedings of EuroSimE, 2009
6. Salmela, O., "Acceleration Factors for Lead-Free Solder Materials", IEEE Transactions on Components and Packaging Technologies, 2007, Vol 30; Numb 4.
7. N. Pan "An acceleration model for Sn-Ag-Cu solder joint reliability under various thermal cycle conditions", Proceeding of SMTAI, 2006.
8. O. Salmela , K. Andersson , A. Perttula , J. Särkkä and M. Tammenmaa "Re-calibration of Engelmaier's model for lead-free solder attachments", Qual. Rel. Eng. Int., vol. 23, 2006
9. Dauksher, W. Lau, J. "A Finite-Element-Based Solder-Joint Fatigue-Life Prediction Methodology for Sn–Ag–Cu Ball-Grid-Array Packages", Device and Materials Reliability, IEEE Transactions on, Volume: 9 Issue: 2, June 2009
10. Chauhan, P. Pecht, M. Osterman, M. Lee, S.W.R., "Critical Review of the Engelmaier Model for Solder Joint Creep Fatigue Reliability", IEEE Transactions on Components and Packaging Technologies, Volume: 32 Issue: 3, Sept. 2009
11. Syed, "Accumulated Creep Strain and Energy Density Based Thermal Fatigue Prediction Models for SnAgCu Solder Joints, Proceedings of ECTC 2004.
12. Kaushik Setty, Ganesh Subbarayan, and Luu Nguyen, "Powercycling Reliability, Failure Analysis and Acceleration Factors of Pb-free Solder Joints", Proceedings of ECTC 2005
13. Jean-Paul Clech, Gregory Henshall, Jian Miremadi, "Closed-Form, Strain-Energy-Based Acceleration Factors for Thermal Cycling of Lead-Free Assemblies", Proceedings of SMTAI October 2009
14. Jean-Paul Clech, "Acceleration Factors and Thermal Cycling Test Efficiency for Lead-Free Sn-Ag-Cu Assemblies", Proceedings of SMTAI, September 2005.

15. Farooq, M., Goldmann, L., Martin, G., Goldsmith, C. and Bergeron, C., "Thermo-Mechanical Fatigue Reliability of Pb-Free Ceramic Ball Grid Arrays: Experimental Data and Life Time Prediction Modeling", Proceedings, 53rd Electronic Components and Technology Conference, New-Orleans, LA, May 2003.
16. Lau, J. H., Shangguan, D., Lau, D. C. Y., Kung, T. T. W. and Lee, S. W. R., "Thermal-fatigue life prediction equation for Wafer-Level Chip Scale (WLCSP) lead-free solder joints on lead-free Printed Circuit Board (PCB)", Proceedings, 54th Electronic Components and Technology Conference, Las Vegas, NV, June 2004.
17. Jianbiao Pan, Jyhwen Wang, David M. Shaddock, "Lead-free Solder Joint Reliability – State of the Art and Perspectives", Proceedings of the 37th International Symposium on Microelectronics, Long Beach, CA, November 14-18, 2004
18. Pan, N., Henshall, G. A., Billaut, F., Dai, S., Strum, M. J., Benedetto, E. and Rayner, J., "An Acceleration Model for Sn-Ag-Cu Solder Joint Reliability Under Various Thermal Cycle Conditions", Proceedings, SMTA International Conference, Chicago, IL, September 2005.
19. Schubert, A., Dudek, R., Auerswald, E., Gollhardt, A., Michel, B. and Reichl, H., "Fatigue Life Models for SnAgCu and SnPb Solder Joints Evaluated By Experiments and Simulation", Proceedings, Electronic Components and Technology Conference, New-Orleans, LA, May 2003.
20. Clech, J-P., "An obstacle-controlled creep model for SnPb and Sn-based lead-free solders", Proceedings, SMTA International (SMTAI) Conference, Chicago, IL, Sept. 2004.
21. Bart Vandeveld, Mario Gonzalez, Paresh Limaye, Petar Ratchev, Jan Vanfleteren, Eric Beyne. "Lead Free Solder Joint Reliability Estimation by Finite Element Modelling Advantages, Challenges and Limitations", Proceedings of IPC Frankfurt, 2004
22. Vasu Vasudevan and Xuejun Fan, "An Acceleration Model for Lead-Free (SAC) Solder Joint Reliability under Thermal Cycling", Proceedings of ECTC 2008
23. Liyu Yang, Joseph B. Bernstein and T. Koschmieder, "Assessment of Acceleration Models Used for BGA Solder Joint Reliability Studies", Microelectronics Reliability, Volume 49, Issue 12, December 2009, Pages 1546-1554
24. Krishna Tunga and Suresh K. Sitaraman, "Microstructure Evolution Based Acceleration Factor Determination for SnAgCu Solder Joints During Thermal Cycling", International Journal of Materials and Structural Integrity Issue: Volume 2, Number 1-2, 2008
25. John Lau, Ricky Lee, and Dongkai Shangguan, "Thermal Fatigue-Life Prediction of Lead-Free Solder Joints", Proceedings of IMECE04 2004 ASME International Mechanical Engineering Congress and Exposition, November 2004, Anaheim, California.
26. Schuber, A., Dudek, R., Auerswald, E., Golhardt, A., Michel, B., Reichl, H., "Fatigue Life Models for SnAgCu and SnPb Solder Joints Evaluated by Experiments and Simulation", IEEE, Electronic Components and Technology Conference, 2003.
27. Robert Darveaux, "The effect of assembly stiffness and solder properties on thermal cycle acceleration factors", THERMINIC, Belgirate, Italy, Sept. 2005
28. Vasu Vasudevan , Xuejun Fan, Tao Liu, and Dave Young, "Slow Cycle Fatigue Creep Performance of Pb-Free (LF) Solders", Proceedings of ECTC 2007.
29. IPC-A-610D, "Acceptability of Electronics Assemblies," Section 8.2.12.4, 8-83, IPC, February 2005.
30. IPC-9701A, "Performance Test Methods and Qualification Requirements for Surface Mount Solder Attachments," IPC, Bannockburn, IL, (2006).